Journal Pre-proof

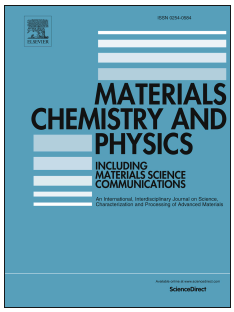

Investigation of high temperature behavior of AlSi10Mg produced by selective laser melting

Carlo Alberto Biffi, Paola Bassani, Jacopo Fiocchi, Donatella Giuranno, Ausonio Tuissi, Enrica Ricci

PII: S0254-0584(20)31335-3

DOI: https://doi.org/10.1016/j.matchemphys.2020.123975

Reference: MAC 123975

To appear in: *Materials Chemistry and Physics*

Received Date: 7 June 2020

Revised Date: 23 September 2020

Accepted Date: 22 October 2020

Please cite this article as: C.A. Biffi, P. Bassani, J. Fiocchi, D. Giuranno, A. Tuissi, E. Ricci, Investigation of high temperature behavior of AlSi10Mg produced by selective laser melting, *Materials Chemistry and Physics*, https://doi.org/10.1016/j.matchemphys.2020.123975.

This is a PDF file of an article that has undergone enhancements after acceptance, such as the addition of a cover page and metadata, and formatting for readability, but it is not yet the definitive version of record. This version will undergo additional copyediting, typesetting and review before it is published in its final form, but we are providing this version to give early visibility of the article. Please note that, during the production process, errors may be discovered which could affect the content, and all legal disclaimers that apply to the journal pertain.

© 2020 Elsevier B.V. All rights reserved.

Journal Pre-proof

Credit author Statement

All the authors: Experimental, data curation and analysis, writing draft and final manuscript.

Journal Pre-proof

Journal Pre-proof

Investigation of high temperature behavior of AlSi10Mg produced by selective laser melting

Carlo Alberto Biffi[1], Paola Bassani[1], Jacopo Fiocchi[1], Donatella Giuranno[2], Ausonio Tuissi[1*] and Enrica Ricci[2]

[1] National Research Council of Italy - Institute of Condensed Matter Chemistry and Technologies for Energy, Unit of Lecco, CNR ICMATE; Via Previati 1/E, 23900 Lecco, Italy.

[2] National Research Council of Italy - Institute of Condensed Matter Chemistry and Technologies for Energy, Unit of Genova, CNR ICMATE; Via de Marini, 6, 16149 Genova, Italy.

Abstract

Among additive manufacturing (AM) processes, Selective Laser Melting (SLM) is the most diffused layer by layer method for manufacturing 3D components. It is based on local melting, induced by a laser scanning, on a powder bed; the limited dimensions of the liquid pool provoke rapid cooling rates which can be associated to significantly finer microstructure than the one obtained by a conventional casting process. Moreover, being the remelting of pre-existing pools, it is of relevant interest to investigate the wettability and the reactivity at high temperature of alloys produced by SLM. In the panorama of alloys for AM, the AlSiMg system is one of the most used, as it belongs to wide family of the Al-Si alloys, extensively used for conventional casting and die-casting technologies, and it offers good weldability. Therefore, the present work has the goal of investigating the high temperature behavior of the SLMed AlSiMg parts. Wettability tests on Al_2O_3 plates were performed considering two different atmospheres (vacuum and Argon) and the contact angle results compared; surface morphology together with the microstructures and the chemical composition variations were analyzed.

Keywords: AlSi10Mg alloy, selective laser melting, wettability, microstructure

Corresponding author: ausonio.tuissi@cnr.it

Journal Pre-proof

Journal Pre-proof

Investigation of high temperature behavior of AlSi10Mg produced by selective laser melting

Carlo Alberto Biffi[1], Paola Bassani[1], Jacopo Fiocchi[1], Donatella Giuranno[2], Rada Novakovic [2], Ausonio Tuissi[1*] and Enrica Ricci[2]

[1] National Research Council of Italy - Institute of Condensed Matter Chemistry and Technologies for Energy, Unit of Lecco, CNR ICMATE; Via Previati 1/E, 23900 Lecco, Italy.

[2] National Research Council of Italy - Institute of Condensed Matter Chemistry and Technologies for Energy, Unit of Genova, CNR ICMATE; Via de Marini, 6, 16149 Genova, Italy.

Journal Pre-proof

Abstract

Among additive manufacturing (AM) processes, the selective laser melting (SLM) is the most diffused layer by layer method to produce 3D components. It is based on local melting of the metallic powder by means of a focused laser source that scanning the powder surface. Hence, the rapid solidification rates of the small liquid pools induce a peculiar microstructure with grains finer than the one obtained by conventional casting processes. Since new layers solidify on top of pre-existing solidified pools, it is definitely interesting to investigate the wettability and the reactivity at high temperature of SLMed alloys. Therefore, the present work has the goal of investigating the high temperature behavior of the widely used AlSiMg alloy, produced by SLM. Wettability tests on Al_2O_3 plates have been performed under two different atmospheres (vacuum and Argon) and the contact angle values compared. In order to assess the reliability of the contact angle data obtained in the present work, the results were analyzed using various predictive models and compared to the literature data. Surface morphology together with the microstructures and the chemical composition variations were analyzed. In particular, surface oxidation and Mg evaporation under vacuum were found to represent the main problems, providing interesting insights on the SLM processing of aluminum alloys.

Journal Pre-proof

Keywords: AlSi10Mg alloy, selective laser melting, wettability, microstructure

Corresponding author: ausonio.tuissi@cnr.it

1. Introduction

Metal-based additive manufacturing (AM), belonging to three-dimensional (3D) printing processes, is a rapidly expanding advanced industrial process, in which high power density heat source is adopted for locally melting a portion of feedstock material for the construction of complex shaped parts. Starting from the CAD file of the original sketch, layer by layer building strategy allows to produce components with high degree of geometrical complexity. Among the different AM technologies, the most diffused is the so-called Selective Laser Melting (SLM), in which a laser beam scans the surface of a thin powder bed for melting it only where the construction of the part is required. By the repetition of the powder melting of the next layers, namely layer by layer building, the realization of the 3D part is allowed [1-2]. The possibility of producing tailored parts or particular forms even with complex geometries that could not be easily obtained by the conventional processes is one of the major advantages of this technology [3, 4].

SLM may be rightfully considered as a rapid solidification metallurgical process because of cooling rates being as high as 10^5-10^6 °C/s. This feature is also connected to the high temperature gradient induced by the small size of the melt pool and the dense energy input locally delivered by the laser source. This out-of-equilibrium condition can in turn induce cellular growth of the material upon solidification, as well as the formation of supersaturated solid solutions and metastable phases, which are far less common in conventionally cast alloys [5-6].

Few metallic compounds can be reliably processed by SLM among them aluminum alloys that are expected to be employed for improving the efficiency of light structural or heat controller parts [7-8]. We focused our attention on AlSi10Mg (Al-9.64Si-0.45Mg, at %) with typical near eutectic composition. Again, it shows good thermal conductivity and high reflectivity [9], good weldability

Journal Pre-proof

[10] and low shrinkage. In addition, due to its good mechanical properties [11-16] AlSi10Mg is widely used for complex shape casting. Furthermore, the age hardening can be induced by precipitation of the Mg_2Si phase, generally known as β phase [17].

Oxidation is certainly one of the drawbacks of AM processing of aluminum alloys [11]. Therefore, oxide formation is a severe impediment to a wettability and can cause defects such as balling. Moreover, the issues related to oxidation during the SLM can be amplified due to the high surface to volume ratio of the micrometric metallic powders. In fact, the control and the correct storage of the powder is an aspect currently investigated for preserving the quality and purity of the feedstock material.

AM process should guarantee low oxidation level to maintain surface properties close to those of the reference alloy [18]. Indeed, it has been shown that although the additive manufacturing process is carried under inert atmosphere, the formation of surface oxide films [8, 19] which can strongly influence the wetting characteristics [20, 21,22] occurs. Several studies on the wettability of aluminum and the influence of oxygen on it have been conducted [23-26], on the contrary, very few data are available on the wettability of AlSiMg alloys. For this purpose, in the present work a study was conducted on the behavior of Al-10Si-0.4Mg (wt %) alloy, hereinafter referred to as the AlSiMg alloy, produced by SLM at high temperature. In order to highlight possible differences with respect to both the conventional cast Al-Si alloy and pure Al, wettability tests were carried out on Al_2O_3 substrates under different environmental conditions. Contact angles obtained from sessile drop tests in two different operative conditions were compared and surface morphology and microstructures of the processed samples were analyzed. The energetics of the liquid AlSiMg/ Al_2O_3 system was described in terms of the contact angle and the work of adhesion combining Butler's, Young's and Dupré's equations [27].

Journal Pre-proof

2. Materials and Methods

2.1 Sample preparation

AlSiMg alloy was processed by SLM (mod. AM250 from Renishaw), starting from powders with mesh size ranging from 20 µm and 63 µm and average size of approximately 45 µm. The powders chemical composition is reported in Table 1. Main SLM parameters, used for the manufacturing of the samples, are listed in Table 2.

Table 1. Chemical composition of the AlSi10Mg powder (wt %)

Si	Mg	Cu	Ni	Fe	Mn	Ti	Al
10	0.4	< 0.25	< 0.05	< 0.25	< 0.1	< 0.15	bal.

Table 2. Process parameters used for the realization of the AlSi10Mg samples

Process parameter	Value
Average power	300 W
Exposure time	120 µs
Spot size	130 µm
Layer thickness	25 µm
Building temperature	25°C
Point distance	130 µm
Hatch distance	140 µm
Atmosphere	Argon

2.2 Wettability measurements

The wetting experiments of SLMed AlSiMg alloy on Al_2O_3 substrate were performed using the classical sessile drop technique [28,29,30]. During such experiments, the time-evolution of the contact angle (θ), liquid metal drop's base radius and the drop's height during the rise of temperature which was measured by a calibrated pyrometer, are monitored.

Journal Pre-proof

The measurements have been performed in ad hoc apparatus consisting of an induction horizontal furnace, heated by an 800 kHz high-frequency generator coupled to graphite heather [18]. The apparatus is provided by a high resolution CCD camera and a specific combined image analysis-software, ad hoc developed (ASTRA view) [19], allowing the liquid metal drop's profile to be acquired.

From the alloy manufactured using SLM process, samples of about 0.2 g were mechanically scratched and then cleaned using the ultrasonic ethanol bath for 5 minutes. Then the alloy sample was placed on a plate of dense Al_2O_3 (Degussit Al25: purity> 99.5% by weight, density> 2.8 g cm^{-3}) with dimensions 1 × 1 cm (surface roughness of Ra = 0.5 μ) and introduced into the center of the furnace. After degassing and kept under vacuum (P_{tot} ~ 10^{-3} Pa) for two hours, the desired atmosphere was imposed, i.e. a vacuum or static inert atmosphere of pure argon gas (99.999%, Argon-Alphagas 2) and heating started. A heating rate of 500 C ° / min was applied to reach the final temperature (T_f). The isothermal conditions were maintained for about 20 minutes before cooling to room temperature.

The wetting behavior of SLMed AlSiMg alloy on Al_2O_3 substrate was tested both under vacuum, characterized by a total pressure P = 10^{-2} Pa, and under a pure Ar- atmosphere, total pressure P=10^5 Pa. The contact angle was measured as a function of time and temperature.

2.3 Surface morphology and microstructure analysis.

The morphology and the chemical composition of upper surfaces and cross sections of the samples subjected to wetting characterization, were analyzed by scanning electron microscopy (FEG-SEM mod. SU70 from Hitachi) and EDXS (mod. UltraDry detector and Noran System Seven suite from Thermo Scientific). After general inspection, performed in order to observe both surface and triple point, the specimens were cut with a metallographic diamond saw along a diameter of the drop and

Journal Pre-proof

polished for the analysis of the cross section. The observations were performed with acceleration voltages in the range 5-15 kV.

3. Results and Discussion

3.1 Experimental results

The characteristic microstructure of SLMed AlSiMg sample, in as built condition, is shown in Figure 1 and Figure 2. Thanks to the high cooling rates reached during the SLM process, supersaturated eutectic Si rich phase is spread into the Al matrix under the form of a continuous cellular network. EDXS results confirm the chemical composition of the Al rich matrix and the Si rich network, respectively.

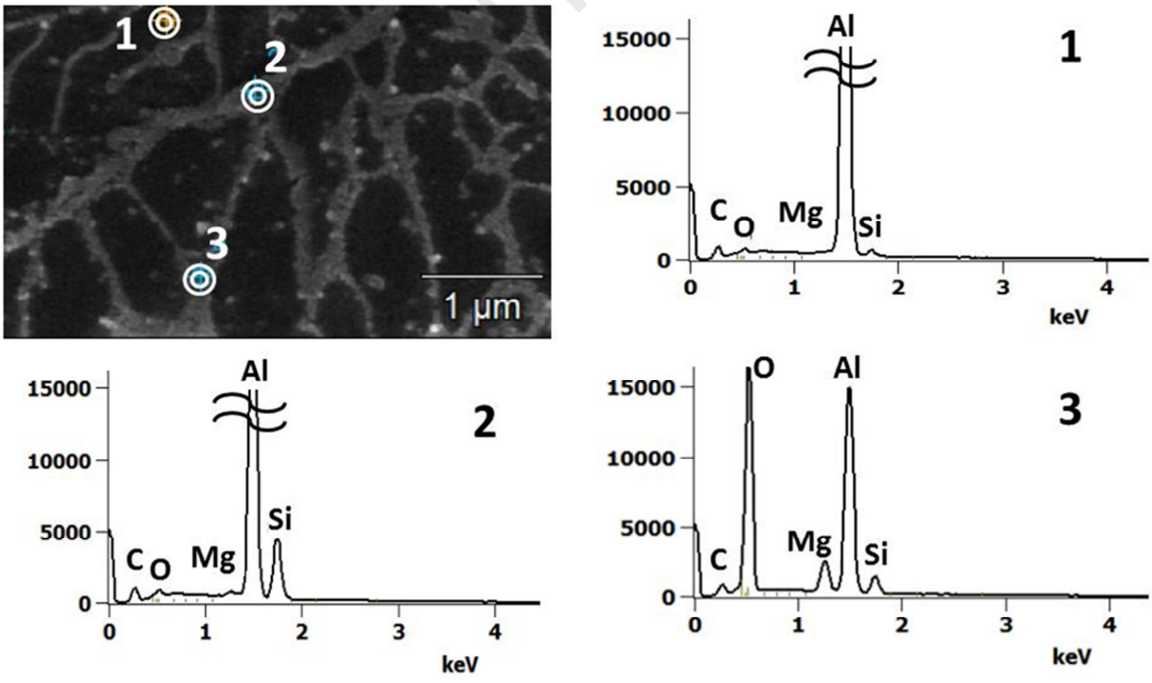

Figure 1. SEM image of SLMed AlSiMg showing the points for EDXS measurements; 1- representative EDX spectra of the Al matrix, 2- the cellular Si rich network, and 3- a thin oxide layer with also Mg. Spectra were cropped at the same count number in order to highlight the difference between Si, O and Mg relative content.

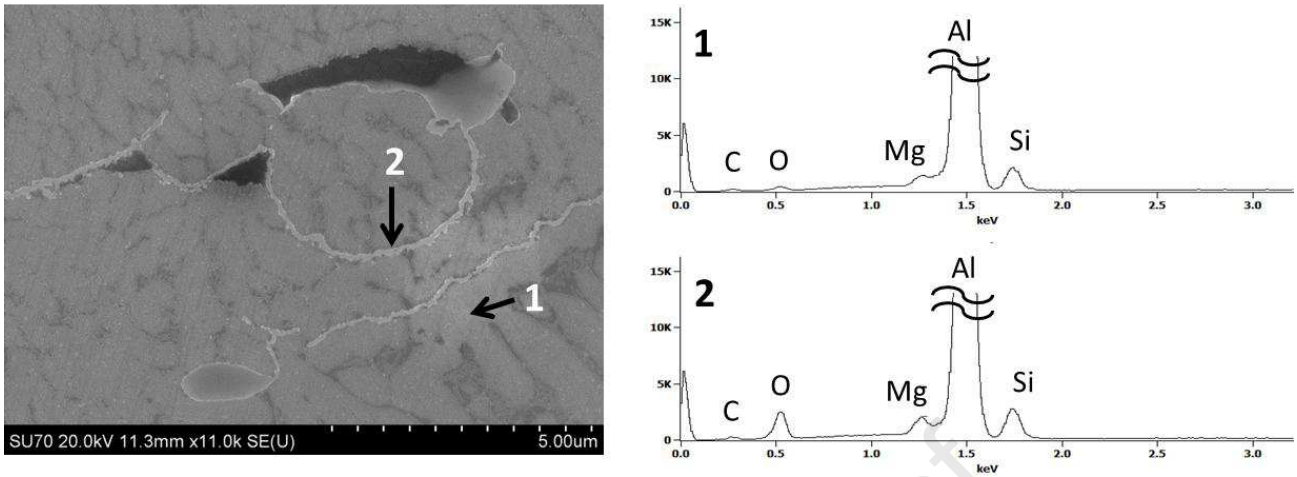

Figure 2. Cross section of the SLMed AlSiMg alloy indicating the presence of oxides layers surrounding previous melting pools or balling liquid (left); EDXS compositional analysis related to the points 1-2. Spectra were cropped at the same count number in order to highlight the difference between O and Mg relative content (right).

A typical microstructure of AMed Al alloys, characterized by primary aluminum columnar grains growing in the direction of thermal gradients and intergranular eutectic structure composed of aluminum and thin branched silicon network was observed (Figure 1). Occasionally, internal oxide layers were observed, characterized by an enrichment of Mg, with respect to the matrix (Figs. 1 and 2). EDXS analyses revealed that even if possibly some Mg could evaporate during SLM process, detectable amount is still present in the processed material.

In Figures 3 the wetting behavior of the SLMed AlSiMg sample on Al_2O_3 substrate measured under vacuum conditions as a function of time and temperature is shown. After about 2-3 minutes from the beginning of the test, the sample started to melt at T≈ 800 °C, but almost simultaneously the surface of the sample stopped emitting, started swelling and rapidly imploded. During this short period of time, a high instability of collected data was observed. After about 5 minutes from the beginning of the test, at T ≈ 1100 °C, the sample started the wetting process again with an initial contact angle value of 140°. Thereafter, the contact angle decreased very rapidly to an average

value of about 88° which remained constant until the end of the test, with a variation of about 9 - 10°.

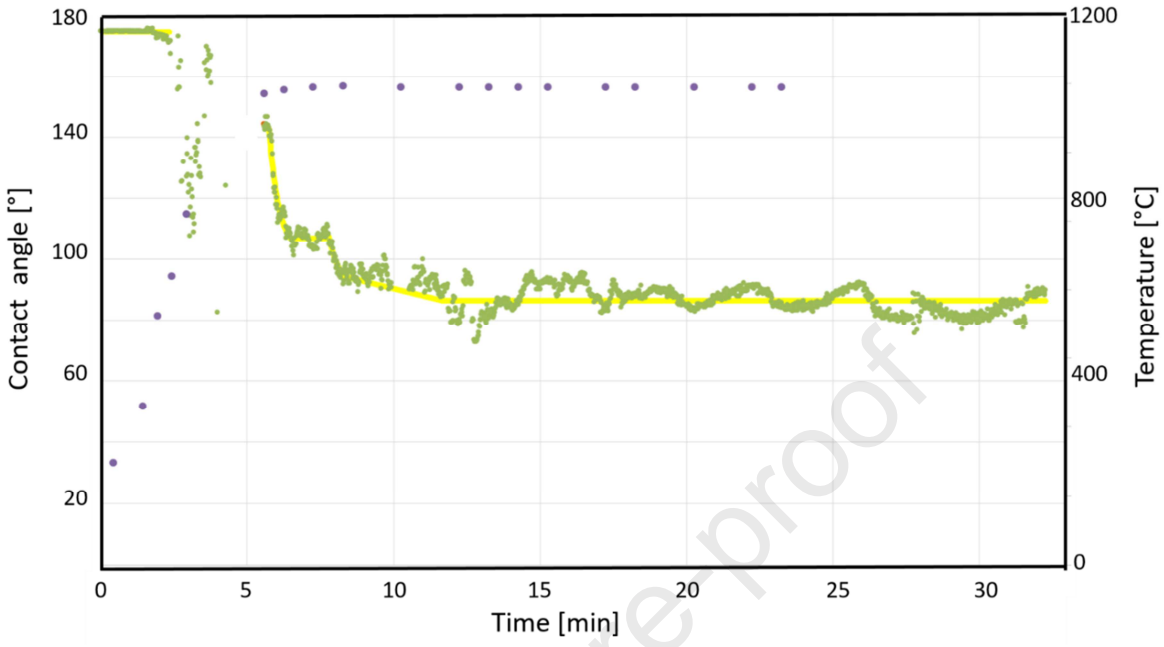

Figure 3. Contact angle versus time of SLMed AlSiMg alloy on Al_2O_3 substrate under vacuum (P= 10^{-2} Pa).

The evolution of the sample during the test is shown in Figure 4.

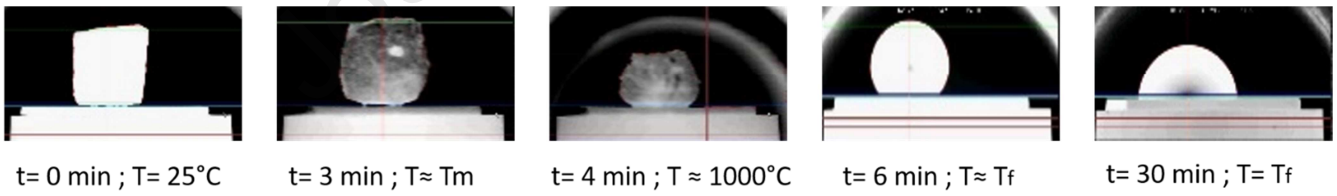

Figure 4. Evolution of the SLMed AlSiMg sample on Al_2O_3 substrate during the wetting test shown in Figure 3 (t= time; T_m = melting temperature; T_f= final temperature).

The solidified sample on the alumina substrate after the wetting test is shown in Figure 5. The low shining indicates the possible formation of surface oxide.

Journal Pre-proof

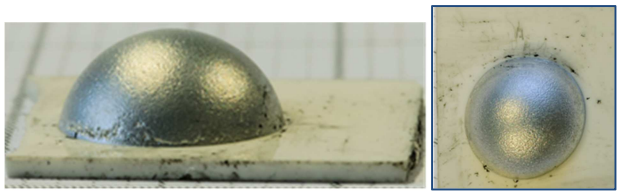

(a) (b)

Figure 5. Lateral (a) and top (b) views of the AlSiMg drop solidified on the Al_2O_3 substrate after the wetting test under vacuum.

The sample was then subjected to SEM-EDXS characterization. In Figures 6 and 7, micrographs of the drop surface of the AlSiMg after the wetting test under vacuum condition, are shown. Typical features are highlighted and corresponding EDXS analyses are reported.

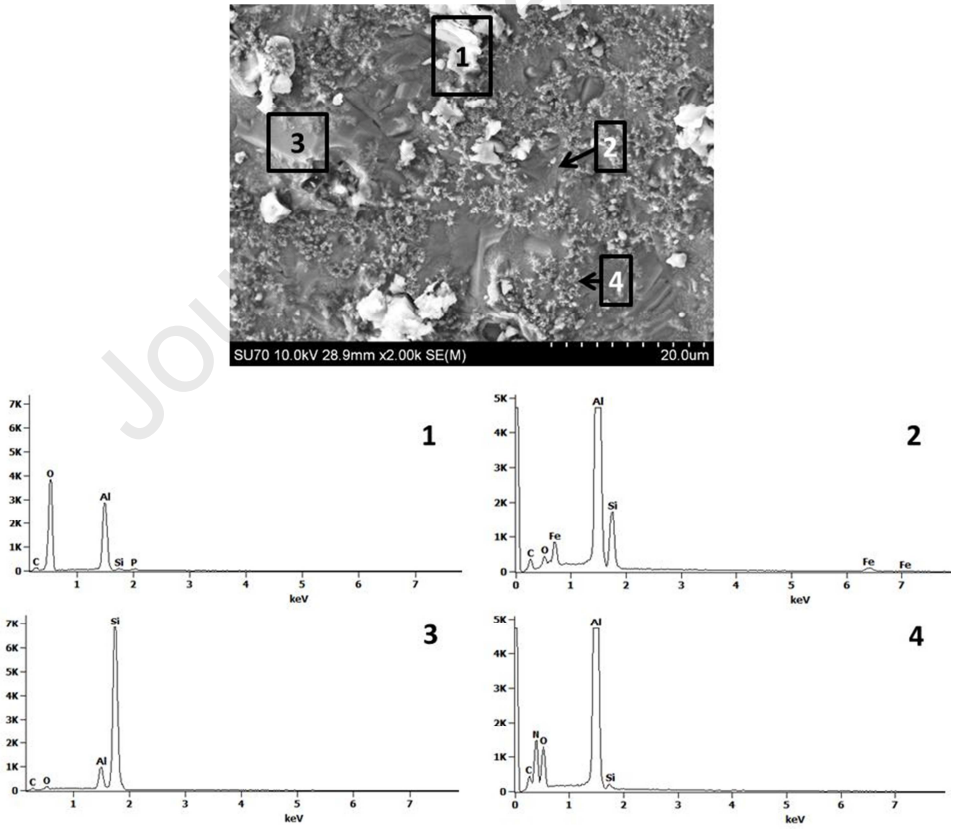

Figure 6. SEM micrograph of the surface of the AlSiMg drop solidified on the Al_2O_3 substrate after the wetting test under vacuum condition, lower part of the specimen. Typical features are highlighted in the micrographs and corresponding EDXS analyses are reported: 1- blocky aluminum oxides, 2- iron rich particles, 3-silicon particles, 4-small globular nitrogen rich aluminum oxides.

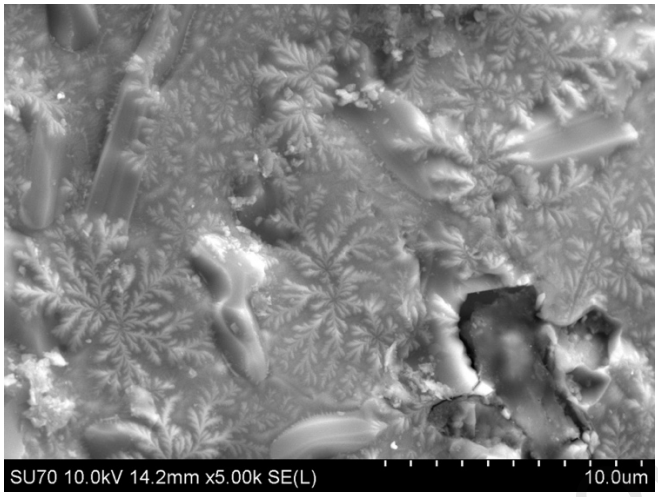

Figure 7. SEM micrograph of the surface of the AlSiMg drop solidified on the Al_2O_3 substrate after the wetting test under vacuum condition: leaf like oxides are visible, together with Silicon particles emerging from inside.

In order to define the chemical composition of the detected compounds with different morphologies and dimensions the EDXS analyses were performed. They can be grouped as follows:

- blocky aluminum oxides: already visible at low magnification, having size of several microns (Figure 6, spectrum n. 1);
- leaf-like aluminum oxides: very thin and detectable only at higher magnification (Figure 7);
- smooth polygonal shapes: they are mostly Silicon particles that solidifies before the rest of the specimen, (primary silicon), and consequently stay in place while the rest of the specimen solidify and retire (Figure 6, spectrum n. 3);
- small globular aluminum oxides: they were observed in the lower part of the specimen and exhibit an unusually high nitrogen content (Figure 6, spectrum n. 4).

Moreover, small iron-rich phases can be observed through BSE micrographs close to silicon particles (Figure 6, spectrum n. 2). EDXS analyses did not reveal the presence of magnesium and /or magnesium oxide neither on the surface of the specimen, nor on the surface of the alumina base. The results of the EDXS analysis suggest that what was observed during the first 5 minutes of

Journal Pre-proof

testing was most of Mg leaving the liquid drop and producing the implosion. This can be attributed to high Mg vapour pressure [31]. Until now there is no data on Mg vapour pressure over liquid Al-Si-Mg alloys, but the corresponding data for liquid Al-Mg alloys with Mg-content varying between 0.035 and 88.7 at %, obtained in the temperature range of 449-913 °C by the Knudsen effusion method have been reported by Moser et al. [32]. Among the data reported in [32], that one related to the Al-0.444Mg (in at %) at T= 837 °C, indicating Mg vapour pressure of 18.59 Pa, may be considered as an estimate for Mg vapour pressure of the SLMed AlSiMg (Al-9.64Si-0.45Mg, in at %) having almost the same Mg-content. In addition, during the measurements of Mg vapour pressure, due to lost vapour, the depletion of Mg-content resulted in changing Al-Mg sample compositions was found [32]. Similar findings were observed in the present study along with concomitant effects of Mg-vaporisation and Al-oxidation (Figure 8).

Thereafter, the sample composition, was reduced to that with nearly only Al and Si, exhibiting the wetting behavior very similar to that observed for the Al-12.6Si (wt%) alloy with comparable final contact angle values [22].

Further, in Figure 8 a low magnification SEM micrograph is shown, where the microstructure of the sectioned AlSiMg alloy is comparable to that of a conventional binary cast alloy [33]. Needles of eutectic Al-Si is clearly seen, highlighting the microstructural variation occurred during the wetting test in comparison to the microstructure of the original alloy (Figures 1 and 2). Additionally, oxidized regions with some residual Mg could be detected. The EDXS analyses performed on selected zones of the sample clearly highlight: b) the Al matrix; c) the presence of Al-Mg oxide and d) the eutectic Al-Si.

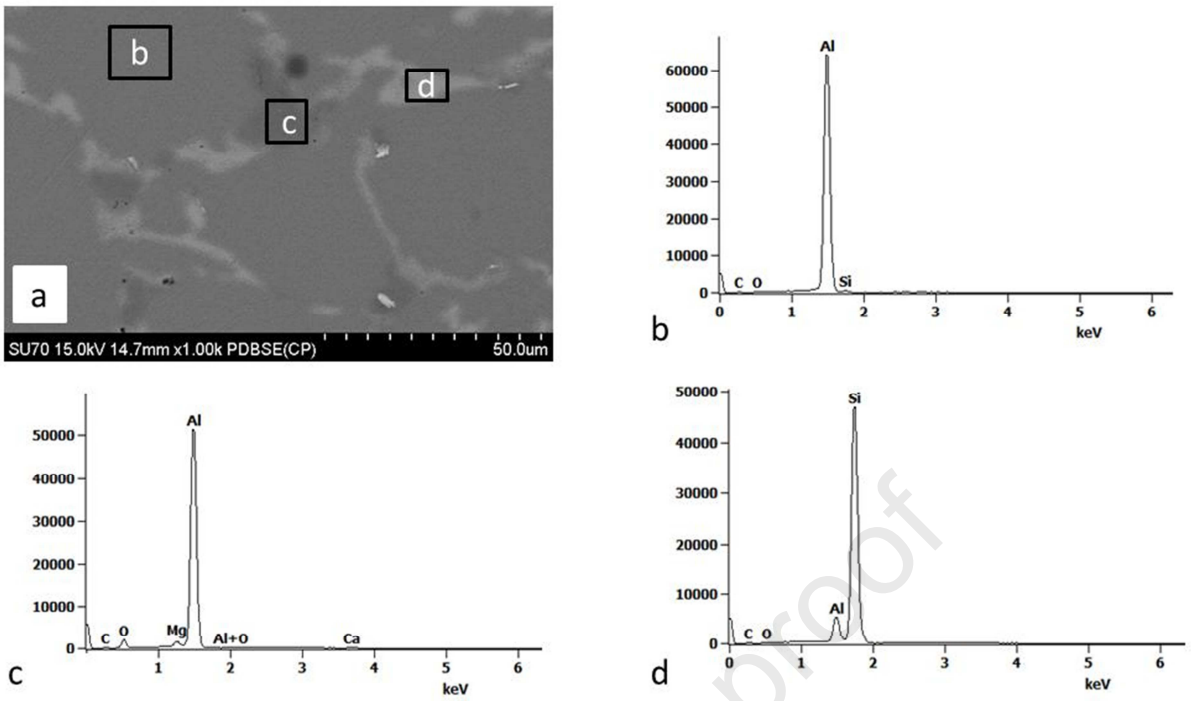

Figure 8. SEM image of the sample's section, showing the EDXS measurement areas (a); EDXS spectra representative of the three regions (b-d).

Different wetting behavior was observed during the test performed under the Ar- atmosphere. In this case, by increasing the temperature, the alloy sample started to show a moderate swelling followed by a sudden shrinkage while maintaining a similar shape to the initial one. In contrast to the previous case, no wetting occurred. Figure 9 shows the temporal evolution of the sample during that test.

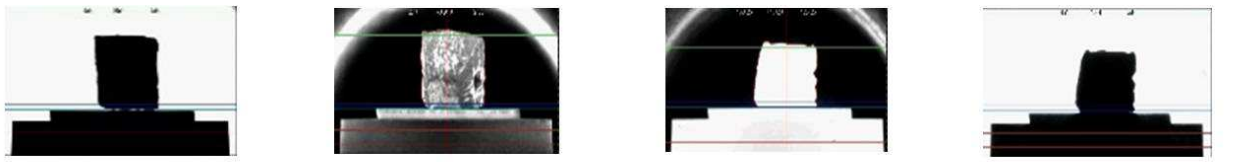

Figure 9. Evolution of the SLMed AlSiMg alloy on Al_2O_3 substrate during the wetting test performed under Ar- atmosphere (t= time; T_m = melting temperature; T_f= final temperature).

Journal Pre-proof

Figure 10 shows the solidified sample just extracted from the furnace at the end of the test performed in Ar-atmosphere. The specimen appeared strongly oxidized. The surface of the sample and the nearby alumina substrate were both covered by a thick layer of oxides. On visual inspection, the surface of the substrate shows different colors indicating oxides of different shapes: a dense forest of branched and leaf-like filaments of oxides are present closer to the sample, while the oxides furthest from the sample are in minor quantity and show a rounded shape.

Figure 10. Image of the SLMed AlSiMg sample solidified on Al_2O_3 substrate, after the wetting test performed under Ar- atmosphere.

The surface of the solidified alloy sample depicted in Figure 10, has been analyzed by SEM/EDXS. The morphology of the sample indicates some macro irregularities, absent in the sample tested under vacuum. The shape is quite irregular: most of the surface is covered by a thick layer of micrometric and even thinner oxides, characterized by irregular shapes, such as filaments and crystals as shown in Figure 11.

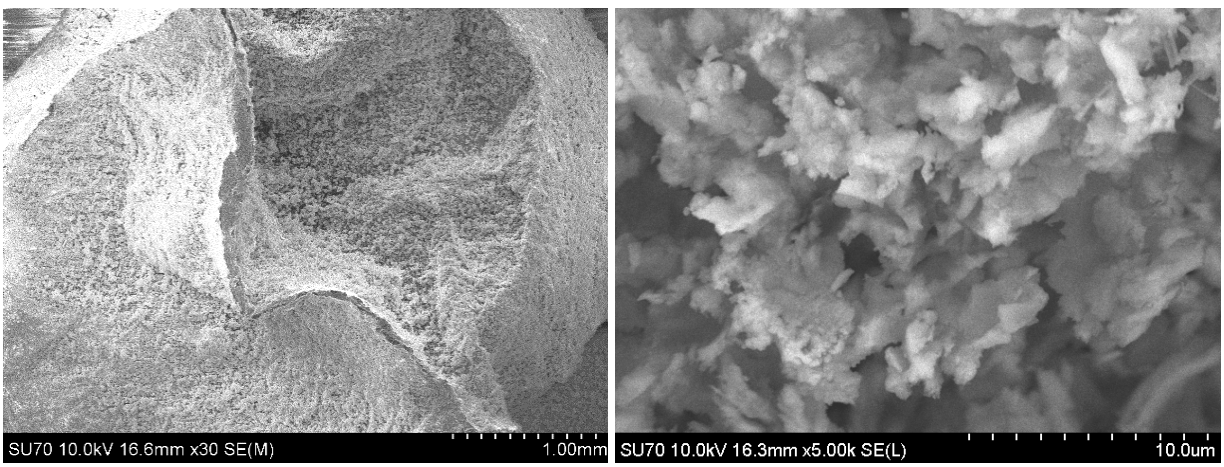

Journal Pre-proof

Figure 11: Micrographs of the drop surface of SLMed AlSiMg alloy on Al_2O_3 substrate after the wetting test performed under Ar- atmosphere low (left) and high (right) magnification.

On the other hand, on the surface of Al_2O_3 substrate, the presence of at least two types of oxides was detected: aluminum oxide with generally hexagonal shape, as indicated by EDXS analysis showing peaks only from Al and O (spectrum 1 in Figure 12), and mixed aluminum and silicon oxide (spectrum 2 in Figure 12), having irregular shapes, similar to filaments, decorated by leaves and pearls.

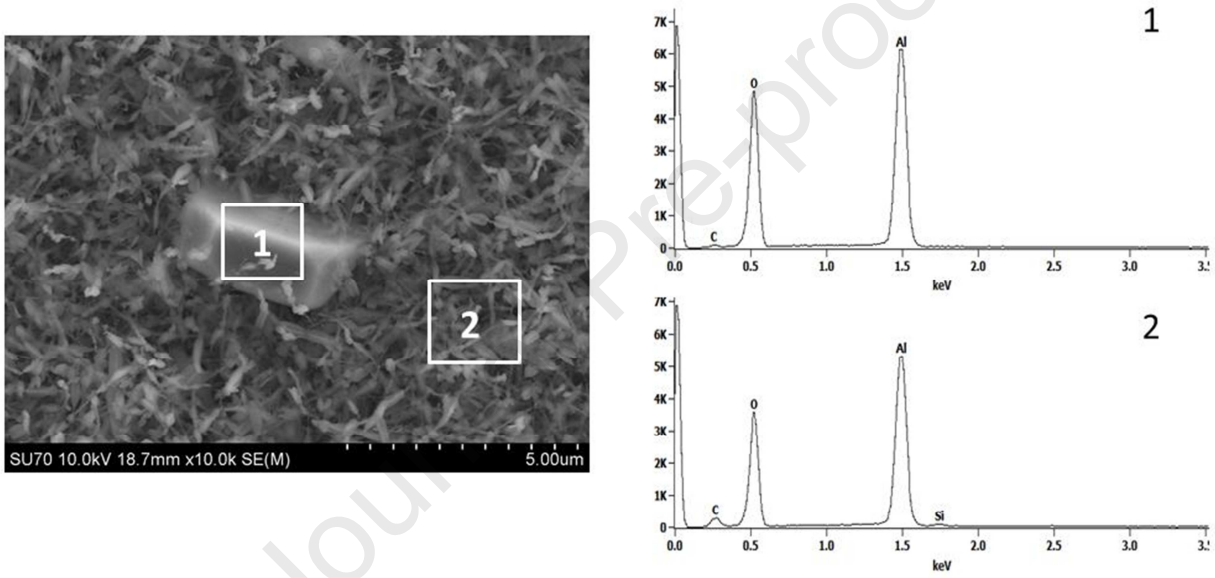

Figure 12. SEM image of the Al_2O_3 substrate after the wetting test performed under Ar-atmosphere; spectrum of the polygonal aluminum oxides (1) and the thin mixed Al-Si oxide (2).

It is well apparent that the two atmospheres produced a strongly different oxidation. A rough estimation of oxygen partial pressure in the two cases indicates that these values differ by three orders of magnitude. If we assume that the residual atmosphere is composed of air, for the evacuate chamber a maximum of $2x10^{-3}$ Pa of oxygen could be present, that is far lower than that in the case of Ar filled. In the latter case possibly up to 0.2-1 Pa of oxygen could be present (residual oxygen in Ar gas, and eventual remnant of air in the chamber). Studies about oxidation of aluminum [34-35] show that aluminum oxide formation is quite enhanced in the range 950-1250°C, where metastable

Journal Pre-proof

Gamma-Al_2O_3 is formed, and become slower at higher temperature, when stable alfa-Al_2O_3 forms. In contrast, wetting experiments conducted in vacuum atmosphere, evidence that at higher temperatures Al_2O_3 film disappears [23]. Due to the paucity of the wettability data of the AlSiMg alloys, the comparison with the few available data of the Al-Si system is necessary. Altought the wetting behaviuor of Al-Si alloys on Al_2O_3 substrate was less investigated than that of Al on Al_2O_3, the contact angle values of Al-Si alloys on Al_2O_3 substrate as a function of composition are reported by Shen et al. [25]. From the data available in [25], the contact angle value $\theta = 73°$ at T=1450 °C was extrapolated for Al-12.6Si eutectic alloy [18], that agrees with the contact angle value measured in this work under a vacuum at T=1100°C. This value is also consistent with those reported in the literature, taking into account the dependence on temperature and the segregating effect of Si. Their effects on the surface properties are discussed in the next section. The poor wettability observed in test carried out under vacuum has to be attributed to surface oxidation which, as is well known, strongly influences the behaviour of the triple line [21]. In addition, the effect of mass exchanges between liquid and working atmosphere under stationary conditions [19] allowing to determine the effective oxygen pressure at which the oxidation of the metal becomes evident, have to be considered. In the particular case of Al, experimental results [36] indicated that oxidation–deoxidation transitions occur at values higher than the thermodynamic ones, owing to the non-negligible contribution of the linked oxygen in the form of Al_2O volatile oxide. During heating, once aluminum melts, if the oxide layer is sufficiently thick, it may prevent the wetting of liquid aluminum on the substrate, and an irregular shape is maintained. It is known that the presence of Al_2O_3 as well oxygen in the atmosphere help stable foam formation for aluminum melt [37]. Accordingly, under the operating conditions applied in this work, the oxidation regime seems to be always established. In fact, in the test under vacuum, although the Knudsen regime was set [24], the de-oxidation conditions were not achieved. The Ar- atmosphere seems to contain sufficient oxygen amount to stabilize the oxide film, and eventually re-oxidize evaporated Al_2O as well as other evaporated elements (Al, Si). This results in the formation of oxides outside the specimen that then

Journal Pre-proof

freeze on the substrate surface: α-Al_2O_3 granules with hexagonal shape were easily found on the substrate, together with aluminosilicates and reasonably mullite, ($3Al_2O_3$-$2SiO_2$ or $2Al_2O_3$-SiO_2) [38, 39], that possesses orthorhombic structure and is generally found in ceramics as filaments.

3.2 Surface tension and segregation calculations

In multicomponent liquid alloys, the alloying elements with lower surface tensions have twofold effects on their surface properties: an enrichment of the melt surface by the atoms of tensioactive elements and a decrease in the surface tension of an alloy. In the case of the Al-Si-Mg system, the surface tension reference datasets of liquid Al, Si and Mg [40] indicate Mg and Si as tensioactive elements. Therefore, as a rule, the segregation of Mg and Si-atoms to the surface of liquid Al-Si-Mg alloys can be expected, as it was observed experimentally for the SLMed AlSiMg (Figure 1 and Figure 2). Due to a very low content of Mg in the SLMed AlSiMg (Al-10Si-0.4Mg, in wt %; Al-9.64Si-0.45Mg, in at %) alloy, its surface properties were further analysed using the model predicted values of the Al-Si system composed of Al and Si major alloying elements [41]. To this aim, the surface tension (σ) of liquid Al-Si alloys was calculated by the Butler model [18], as follows:

$$\sigma = \sigma_i + \frac{RT}{S_i}\ln\left(\frac{C_i^s}{C_i^b}\right) + \frac{1}{S_i}\left[G_i^{xs,s}(T, C_i^s) - G_i^{xs,b}(T, C_i^b)\right] \qquad (i = A, B) \qquad \text{(Eq. 1)}$$

where R, S_i, C_i^b, C_i^s, $G_i^{xs,b}$, $G_i^{xs,s}$ are gas constant, surface area, composition and partial excess Gibbs free energy of a component i in the bulk and surface phases, respectively. The energetic terms have the same functional form; both are temperature and composition dependent and $G_i^{xs,s}$ is proportional to $G_i^{xs,b}$ by means of reduced coordination, expressed as the ratio between the coordination numbers of the surface and the bulk phase. To calculate the surface tension and the surface segregation isotherms, the Gibbs free energy of the Al-Si liquid phase [42], molar volume,

Journal Pre-proof

structural data [40] and the surface tension data of the pure components Al [43] and Si [44] were taken as input data. The effects of Mg on the surface tension and the surface segregation of the SLMed AlSiMg alloy were evaluated by comparison with the corresponding values of the Al89.91-Si10.09 alloy having the same Al-content as the Al-9.64Si-0.45Mg (Figure 13 and Figure 14).

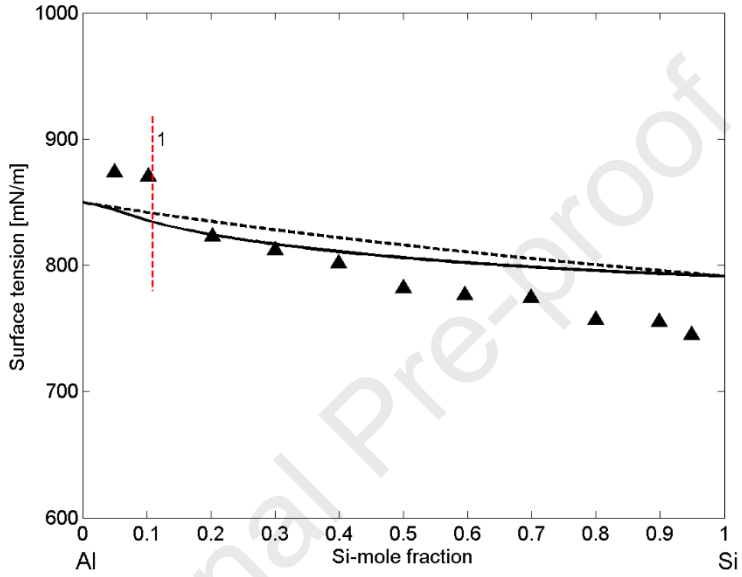

Figure 13. Surface tension isotherms of liquid Al-Si alloys calculated for T=1100 °C (full line – Butler's model; dashed line – the ideal solution model) together with the literature data (▲) [45]. For a comparison, an estimation of the surface tension of the Al-10Si-0.4Mg (Al-9.64Si-0.45Mg, in at %) given by the surface tension calculated value of the Al89.91-Si10.09 (line 1 – compositional location of the Al89.91-Si10.09 alloy).

The surface tension of the Al89.91-Si10.09 calculated for T=1100 °C by the Butler model is σ = 836 mN/m (Fig. x1a, line1), while for the Al90-Si10 alloy with slightly different composition, the experimental value of σ = 870 ± 43 mN/m having the experimental error of 5 % was reported [45]. To the best of our knowledge, the Al-Si-Mg system has no ternary compound [46, 47] and, as in the case of its basic Al-Si binary subsystem, it may be assumed that the realistic surface tension

values of these ternary alloys are lower than those of their ideal mixture. A rough estimate of the surface tension of the SLMed AlSiMg can be calculated using a weighted sum of the surface tension reference values each multiplied by the corresponding content of the alloying element. Considering the surface tension data of liquid Al [41], Si [44] and Mg [31], for the Al-9.64Si-0.45Mg at T=1100 °C, the value of σ = 842 mN/m is obtained.

Therefore, an estimation of the surface tension of the SLMed AlSiMg equal to σ = 835 mN/m may be considered as reliable.

The calculations of the surface segregation of liquid Al-Si alloys indicate for all alloy compositions and temperatures the enrichment of the melt by Si-atoms [18], as it was also experimentally observed by the microstructural analysis, performed after the wetting tests on the SLMed AlSiMg / Al_2O_3 couple (Figures 1,2 and 8). The degree of Si-segregation is temperature dependent, and at T=1100 °C is not pronounced (Figure 14).

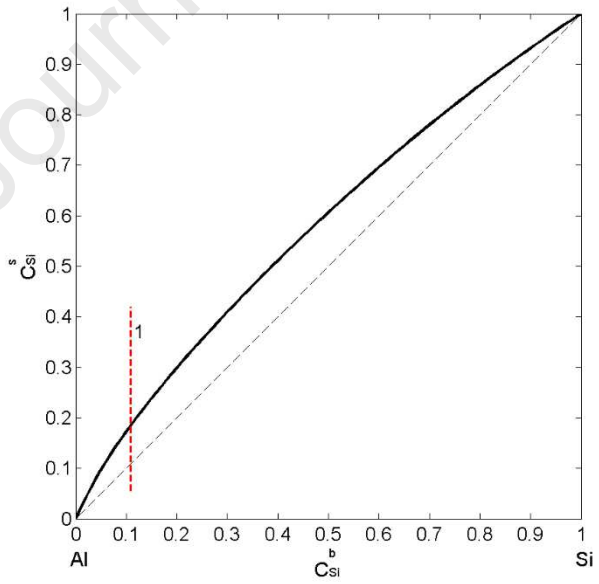

Figure 14. Surface segregation isotherms of liquid Al-Si alloys calculated for T=1100 °C (full line – Butler's model; dashed line – the ideal solution model). For a comparison, an estimation of the surface enrichment of the Al-10Si-0.4Mg (Al-9.64Si-0.45Mg, in at %) given by the corresponding value of the Al89.91-Si10.09 alloy (line 1 – compositional location of the Al89.91-Si10.09).

Journal Pre-proof

The energetics of metal/ceramic systems characterised by non-reactive wetting is defined in terms of the contact angle and work of adhesion. In order to evaluate the energetics of the liquid Al-10Si-0.4Mg/ Al_2O_3 system, the first step is to calculate the interfacial energy (σ_{LS}) between the liquid and the solid phase. To this aim, the new experimental contact angle value, the predicted surface tension value of the Al-10Si-0.4Mg and literature data of the surface energy of solid Al_2O_3 [48] were inserted into Young's equation [28] resulting in σ_{LS} = 1.371 J/m^2. The work of adhesion W_A = 0.874 J/m^2 is obtained by Dupre's equation [28]. The values obtained for this system are of the same magnitude as those found for similar systems [27].

4. Conclusions

The study of the behavior of Al-10Si-0.4Mg (wt. %) alloy, produced by SLM, at high temperature by performing wettability tests on Al_2O_3 substrates under different environmental conditions has been carried out. The results obtained and the analyses of surface morphology and microstructures of the processed samples lead to the following conclusions:

- Poor wettability with high instability of the contact angle values under vacuum conditions was observed. In Ar- atmosphere, despite the purity of the gas associated with the presence of reducing elements such as the graphite susceptor, no reliable contact angle data have been obtained due to the strong surface oxidation.

- Evaporation of Mg and the consequent microstructural variation occurred during the wetting tests under a vacuum, lead to a microstructure of the AlSiMg alloy comparable to that of a conventional cast binary alloy;

- Accordingly, the wetting behavior of AlSiMg alloy under vacuum is very similar to that observed for the Al-12.6Si (wt%) alloy under the same operative conditions, with comparable final contact angle values;

Journal Pre-proof

- Surface properties of the Al-10Si-0.4Mg can be evaluated by Butler's equation and are very close to those of the reference Al-Si binary alloy;

- In order to reduce/prevent the strong tendency to oxidation of Al-based alloys which represents one of the main obstacles to the widespread use of Al-based alloys for the SLM process in AM, an implementation of the SLM process by control and monitoring of the oxygen content is required.

Acknowledgements

Authors wish to thank Michika Takashi of the Dept. of Materials Science and Engineering Tokyo Institute of Technology for her valuable work on the wettability data processing and Mr. F. Mocellin, CNR-ICMATE Genova for the support to the experiments

References

[1] T. Kimura and T. Nakamoto, Microstructures and Mechanical Properties of Al–10%Si–0.4%Mg Fabricated by Selective Laser Melting, J. Jpn. Soc. Powder Metall., 2014, 61, p 531-537, doi.org/10.2497/jjspm.61.531

[2] D. Gu, W. Meiners, K. Wissenbach and R. Poprawe, Laser additive manufacturing of metallic components: materials, processes and mechanisms, Int. Mater. Rev., 2012, 57(3), p 133-164, 10.1179/1743280411Y.0000000014

[3] T. DebRoy, H.L. Wei, J.S. Zuback et al., Additive manufacturing of metallic components – Process, structure and properties, Prog. Mater. Sci., 2018, 92, p 112-124.

[4] J. Martin, B. Yahata, J. Hundley et al., 3D printing of high-strength aluminum alloys, Nature, 2017, 549, p 365-369, 10.1038/nature23894

[5] J. Fiocchi, C.A. Biffi, P. Bassani and A. Tuissi, Tailored thermal treatment for SLM built aluminium alloy product, International Powder Metallurgy Congress and Exhibition, Milan, Italy, 1-4 October 2017, Code140833.

Journal Pre-proof

Journal Pre-proof

[6] C.A. Biffi, J. Fiocchi, P. Bassani and A. Tuissi, Continuous wave vs pulsed wave laser emission in selective laser melting of AlSi10Mg parts with industrial optimized process parameters: Microstructure and mechanical behaviour, Addit. Manuf., 2018, 24, p 639-646, 10.1016/j.matdes.2020.108581

[7] M. Wong, S. Tsopanos, C. J. Sutcliffe and I. Owen, Selective laser melting of heat transfer devices, Rapid Prototyping Journal, Rapid Prototyping, 2017, 13(5), p 291-297, 10.1108/13552540710824797

[8] E. Louvis, P. Fox and C. J. Sutcliffe, Selective laser melting of aluminium components, J. Mater. Process. Technol., 201, 211(2), p 275-284, 10.1016/j.jmatprotec.2010.09.019

[9] F. Abe, K. Osakada, M. Shiomi, K. Uematsu and M. Matsumoto, The manufacturing of hard tools from metallic powders by selective laser melting, J. Mater. Process. Technol., 2001, 111, p 210-213, 10.1016/S0924-0136(01)00522-2

[10] C.A. Biffi, J. Fiocchi and A. Tuissi, Laser Weldability of AlSi10Mg Alloy Produced by Selective Laser Melting: Microstructure and Mechanical Behaviour, J. Mater. Eng. Perform., 2019, 28 (11), p 6714-6719, 10.1007/s11665-019-04402-7

[11] N.T. Aboulkhair, I. Maskery, C. Tuck, I. Ashcroft and N.M. Everitt, The microstructure and mechanical properties of selectively laser melted AlSi10Mg: The effect of a conventional T6-like heat treatment, Mater. Sci. Eng. A, 2019, 667, p 139-146, 10.1016/j.msea.2016.04.092

[12] J. Wu, X.Q. Wang, W. Wang, M.M. Attallah and M.H. Loretto, Microstructure and strength of selectively laser melted AlSi10Mg, Acta Mater., 2016, 117, p 311-320, 10.1016/j.actamat.2016.07.012

[13] H. Zhang, H. Zhu, T. Qi, Z. Hu and X. Zheng, Selective laser melting of high strength Al–Cu Mg alloys: Processing, microstructure and mechanical properties, Mater. Sci, Eng. A, 2016, 656, p 47-54, 10.1016/j.msea.2015.12.101

[14] K.G. Prashanth, S. Scudino, H.J. Klauss, K.B. Surreddi, L. Löber, Z. Wang, A.K. Chaubey K, U. Kühn and J. Eckert J., Microstructure and mechanical properties of Al-12Si produced by

Journal Pre-proof

selective laser melting: Effect of heat treatment, Mater. Sci. Eng. A, 2016, 590, p 153-160, 10.1016/j.msea.2013.10.023

[15] N. Read, W. Wang, K. Essa and M.M. Attallah, Selective laser melting of AlSi10Mg alloy: Process optimisation and mechanical properties development, Mater. Des., 2015, 65, p 417-424, 10.1016/j.matdes.2014.09.044

[16] D. Manfredi, F. Calignano et al., Additive Manufacturing of Al Alloys and Aluminium Matrix Composites (AMCs). In: Monteiro WA (editor) InTech, 2014, pp. 3-34, doi:10.5772/58534

[17] D. Buchbinder, W. Meiners and K. Wissenbach, Selective laser melting of aluminum die-cast alloy- Correlations between process parameters, solidification conditions, and resulting mechanical properties, J. Las. App., 2015, 2, S29205, 10.2351/1.4906389

[18] M. Takahashi, D. Giuranno, E. Ricci, E. Arato, R.M Novakovic, Surface Properties of Liquid Al-Si Alloys, Metall. Mater. Trans. A., 2019, 50, p 1050-1060, 10.1007/s11661-018-5054-9

[19] E. Ricci, E. Arato, A. Passerone and P. Costa, Oxygen tensioactivity on liquid-metal drops, Adv. Colloid and Interface Sci., 2005, 117 (1-3), p 15-32, 10.1016/j.cis.2005.05.007

[20] V. Sarou-Kanian, F. Millot, J.C. Rifflet, Surface tension and density of oxygen-free liquid aluminum at high temperature. Int. J. of Thermophys., 2003, 24 (1), p 277–286, 10.1023/A:1022466319501

[22] G. Levi, W.D. Kaplan, Oxygen induced interfacial phenomena during wetting of alumina by liquid aluminium. Acta Mater., 2002, 50 (1), p 75–88, 10.1016/S1359-6454(01)00333-0

[22] Gu Dongdong, Laser Additive Manufacturing of High-Performance Materials, Springer- Berlin Heidelberg, 2015, ISBN 978-3-662-46088-7

[23] S. Bao, K. Tang, A. Kvithyld, M.Tangstad, A. Engh, Wettability of Aluminum on Alumina. Metall. Mater. Trans. B, 2011, 42B, p.1358 – 1366, DOI: 10.1007/s11663-011-9544-z

[24] N. Sobczak, R. Asthana, W. Radziwill, R. Nowak, A. Kudyba, The Role of Aluminum Oxidation in the Wetting-Bonding Relationship of Al/Oxide Couples, Archives of Metallurgy and Materials, 2007, 52, p.55-65.

Journal Pre-proof

[25] P. Shen, H. Fujii, T. Matsumoto, K. Nogi, Critical Factors Affecting the Wettability of α-Alumina by Molten Aluminum, Journal of the American Ceramic Society, 2004, 87, p.1265-1269, 10.1111/j.1151-2916.2004.tb07721.x

[26] J.G Li, Wetting of Ceramic Materials by Liquid Silicon. Aluminum and Mettalic Melts Containing Titanium and Other Reactive Elements: A Review, Ceramic International, 1994, 20 p. 391-412, 10.1016/0272-8842(94)90027-2

[27] R. Novakovic, E. Ricci, M.L. Muolo, D. Giuranno, A. Passerone, On the application of modelling to study the surface and interfacial phenomena in liquid alloy–ceramic substrate systems Intermetallics, 11, 2003, p 1301-1311.

[28] N. Eustathopoulos, M. Nicholas and B. Drevet, Wettability at high temperatures, 1st edn., Pergamon Materials Series ,1999, vol. 3, Oxford.

[29] N. Eustathopoulos, N. Sobczak, A. Passerone and K. Nogi, Measurement of contact angle and work of adhesion at high temperature, J. Mater. Sci., 2005, 40, p 2271-2280, 10.1007/s10853-005-1945-4

[30] A. Passerone and E. Ricci, High Temperature tensiometry, Stud. Interface Sci., 1998, 6, p 475-524, 10.1016/S1383-7303(98)80027-6

[31] Iida, T., Guthrie, R.I.L.: The Physical Properties of Liquid Metals,1993, Clarendon Press, Oxford.

[32] Z. Moser, W. Zakulski, K. Rzyman, W. Gasior, Z. Panek, I. Katayama, T. Matsuda, Y. Fukuda, T. Iida, Z. Zajaczkowski, J. Botor, New Thermodynamic Data for Liquid Aluminum-Magnesium Alloys from emf, Vapor Pressures, and Calorimetric Studies, J. Phase Equilibria, 1998, 19(1), p 38-47, 10.1007/s11669-006-5003-y

[33] I.J. Polmear, Light alloys: metallurgy of the light metals, 3rd ed, John Wiley & Sons Australia, 1995.

Journal Pre-proof

[34] M.A. Trunov, M. Schoenitz, X. Zhu and E.L. Dreizin, Effect of polymorphic phase transformations in Al_2O_3 film on oxidation kinetics of aluminum powders, Combust. Flame, 2015, 140(4), p 310-318, 10.1016/j.combustflame.2004.10.010

[35] M. Schoenitz, B. Patel, O. Qgboh and L. Dreizin, Oxidation of aluminum powders at high heating rates, Thermochim. Acta, 2010, 507(508), p 115-122, 10.2514/6.2009-5080

[36] D. Giuranno, E. Ricci, E. Arato and P. Costa, Dynamic surface tension measurements of an aluminium–oxygen system, Acta Mater., 2006, 54, p 2625-2630, 10.1016/j.actamat.2006.02.005

[37] N. Babcsán, D. Leitlmeier and H.P. Degischer, Foamability of Particle Reinforced Aluminum, Melt. Mat.-wiss. u. Werkstofftech. 2003, 34, p 22-29, 10.1002/mawe.200390011

[38] E.O. Olakanmi, R.F. Cochrane and K.W. Dalgarno, A review on selective laser sintering/melting (SLS/SLM) of aluminium alloy powders: Processing, microstructure, and properties, Prog. Mater. Sci., 2015, 74, p 401-477, 10.1016/j.pmatsci.2015.03.002

[39] H. Schneider, R.X. Fischer and J. Schreuer, Crystal Structure and Related Properties, J. Am. Ceram. Soc., 2015, 98, p 2948-2967, 10.1111/jace.13817

[40] K.C. Mills, Y.C. Su, Review of surface tension data for metallic elements and alloys: Part 1-Pure metals, Int. Mater. Rev. 51(6), 2006, p 329-351, 10.1179/174328006X102510

[41] M. Mohr, R. Wunderlich, R. Novakovic, E. Ricci, H.-J. Fecht, Precise Measurements of Thermophysical Properties of Liquid Ti-6Al-4V (Ti64) Alloy On Board the International Space Station, Adv. Eng. Mater., 22, 2020, 2000169 (pp.1-10), 10.1002/adem.202000169

[42] C.Y. He, Y. Du, H.L. Chen, H. Xu, Experimental investigation and thermodynamic modeling of the Al-Cu-Si system, Calphad, 33(1), 2009, p. 200-210, 10.1016/j.calphad.2008.07.015

[43] J.M. Molina, R. Voytovych, E. Louis, N. Eustathopoulos, The surface tension of liquid aluminium in high vacuum: The role of surface condition, Int. J. Adhesion & Adhesives, 27, 2007, p 394-401, 0.1016/j.ijadhadh.2006.09.006

Journal Pre-proof

[44] S. Amore, D. Giuranno, R. Novakovic, E. Ricci, R. Nowak, N. Sobczak, Thermodynamic and surface properties of liquid Ge-Si alloys, Calphad, 44, 2014, p. 95-101, 10.1016/j.calphad.2013.07.014

[45] H. Kobatake, J. Brillo, J. Schmitz, P.-Y. Pichon, Surface tension of binary Al-Si liquid alloys, J. Mater. Sci. 50, 2015, p 3351-3360, 10.1007/s10853-015-8883-6

[46] H. Feutel, T. Goedecke, H.L. Lukas, F. Sommer, Investigation of the Al-Mg-Si system by experiments and thermodynamic calculations, J. Alloys & Compds 1997, 247, p 31-42, 10.1016/S0925-8388(96)02655-2

[47] Y. Tang, Y. Du, L. Zhang, X. Yuan, G. Kaptay, Thermodynamic description of the Al-Mg-Si system using a new formulation for the temperature dependence of the excess Gibbs energy, Thermochim. Acta, 527, 2012, p 131-142, 10.1016/j.tca.2011.10.017

[48] P. Nikolopoulos, Surface, grain-boundary and interfacial energies in Al_2O_3 and Al_2O_3-Sn, Al_2O_3-Co systems, J. Mater. Sci., 1985, 20, p 3993-4000, 10.1007/BF00552390

Journal Pre-proof

Journal Pre-proof

Table 1. Chemical composition of the AlSi10Mg powder (wt. %)

Si	Mg	Cu	Ni	Fe	Mn	Ti	Al
10	0.4	< 0.25	< 0.05	< 0.25	< 0.1	< 0.15	bal.

Table 2. Process parameters used for the realization of the AlSi10Mg samples

Process parameter	Value
Average power	300 W
Exposure time	120 µs
Spot size	130 µm
Layer thickness	25 µm
Building temperature	25°C
Point distance	130 µm
Hatch distance	140 µm
Atmosphere	Argon

Journal Pre-proof

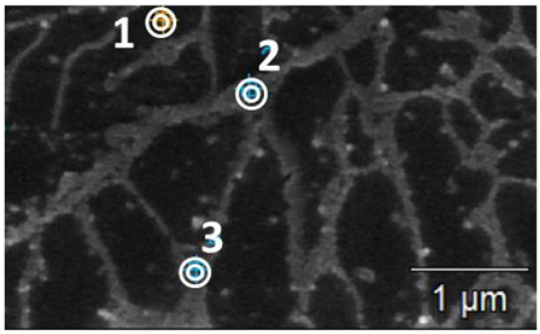

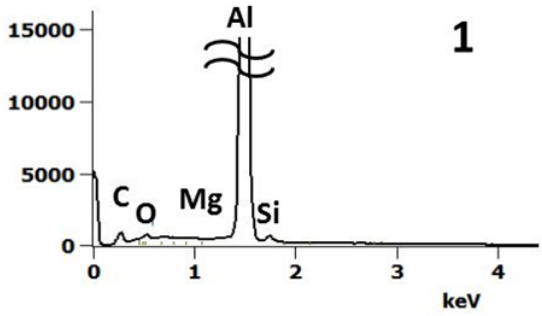

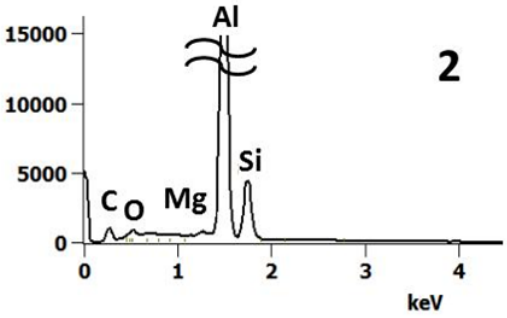

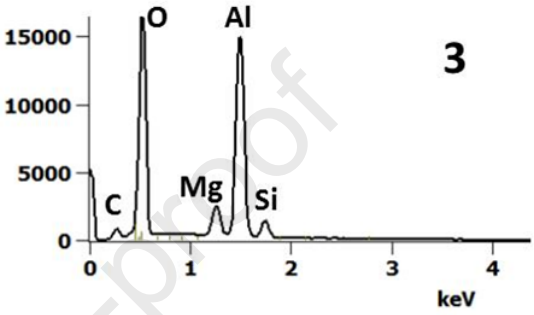

Journal Pre-proof

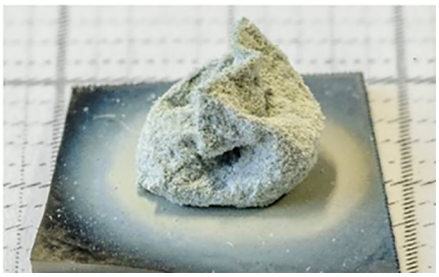

Journal Pre-proof

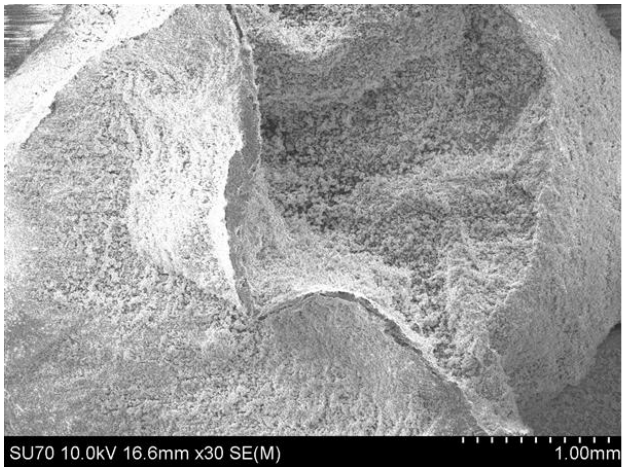

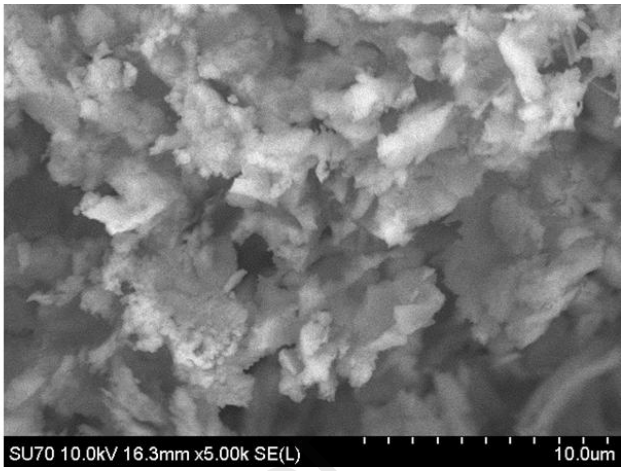

Journal Pre-proof

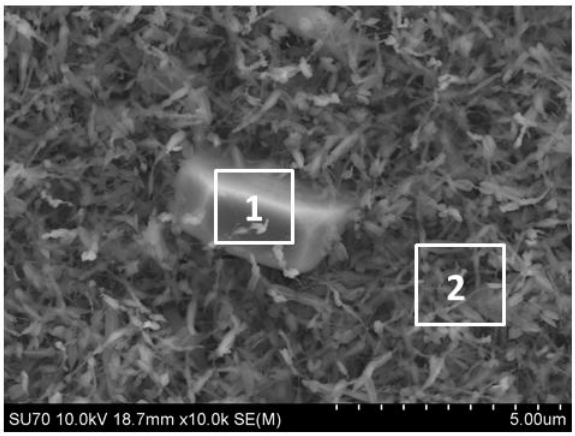

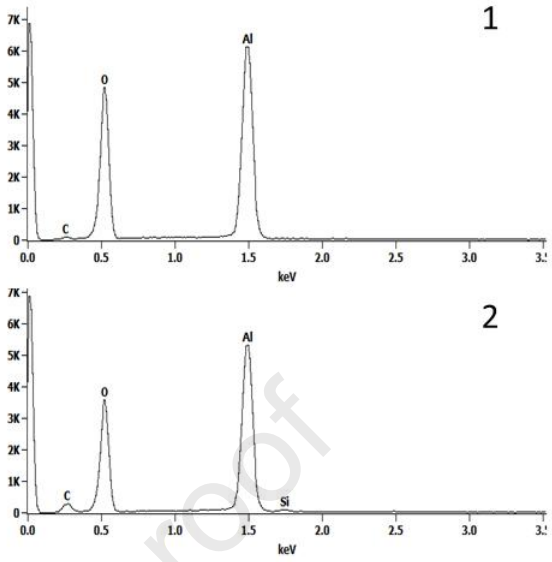

Journal Pre-proof

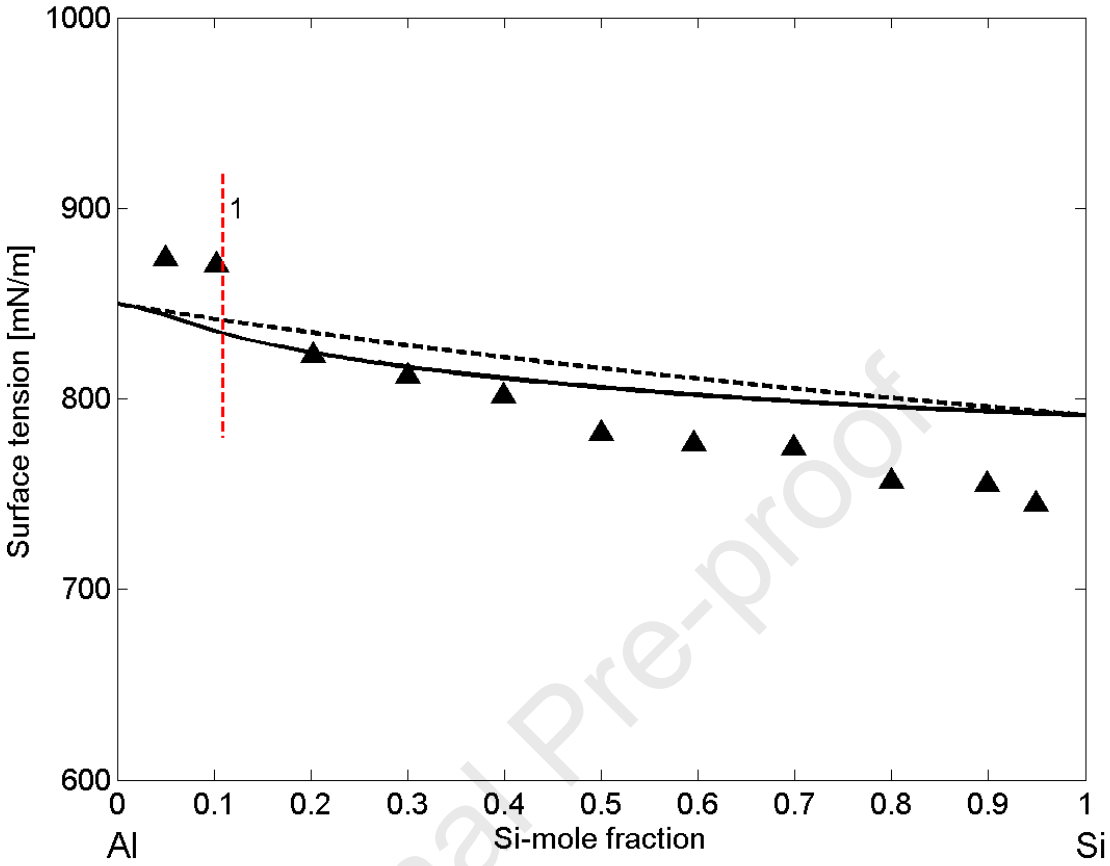

Journal Pre-proof

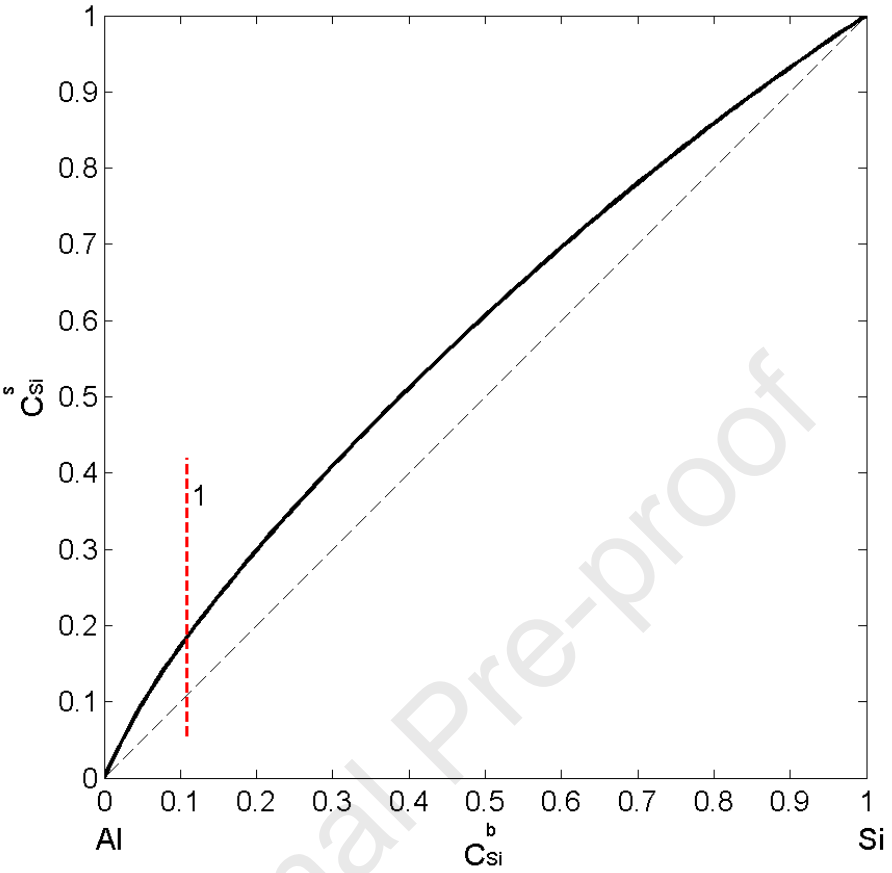

Journal Pre-proof

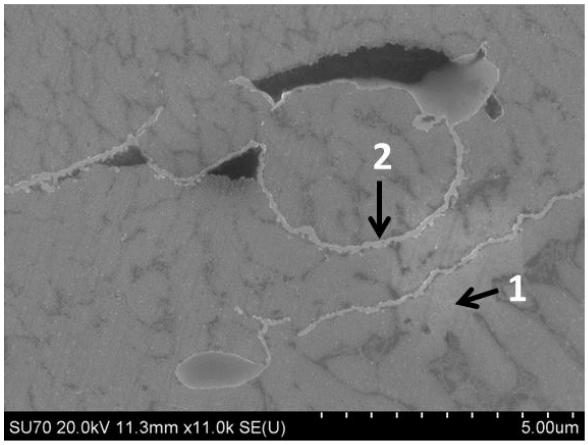

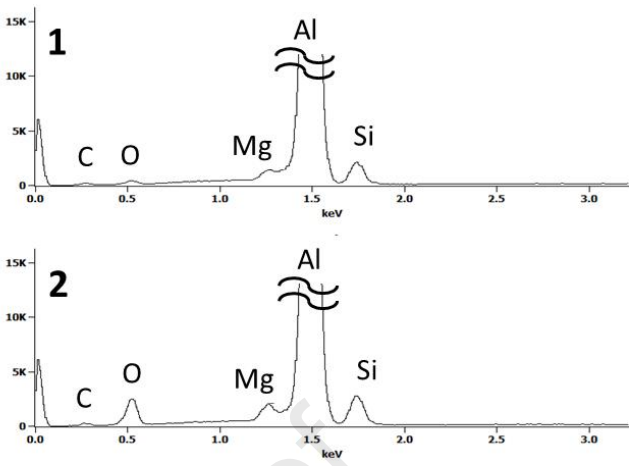

Journal Pre-proof

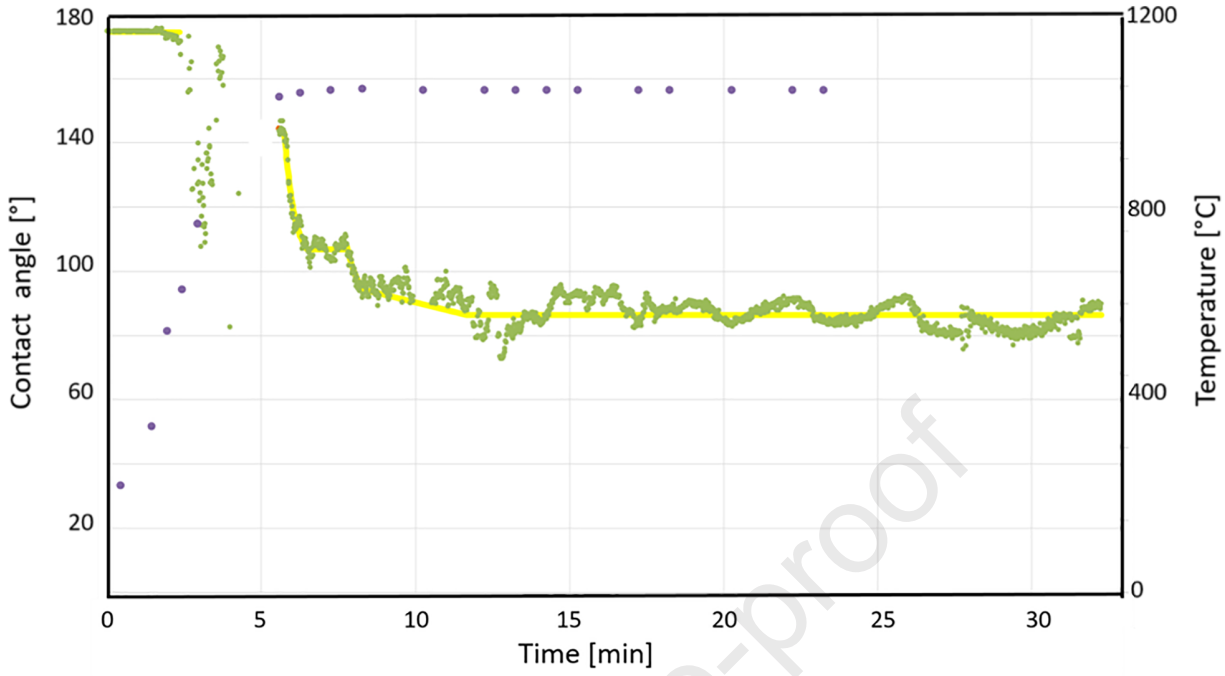

Journal Pre-proof

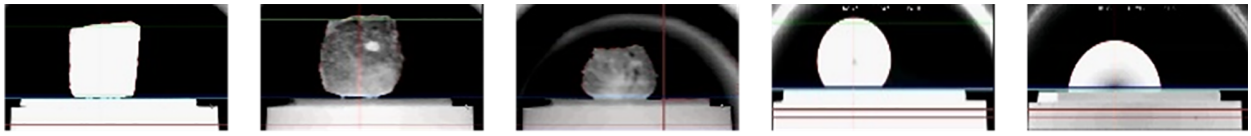

t= 0 min ; T= 25°C t= 3 min ; T≈ Tm t= 4 min ; T ≈ 1000°C t= 6 min ; T≈ T_f t= 30 min ; T= T_f

Journal Pre-proof

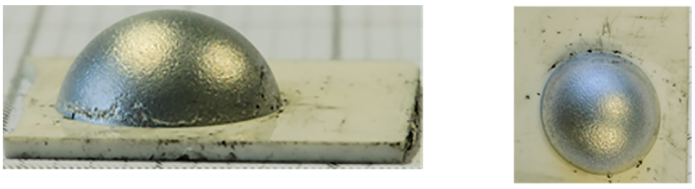

(a)

(b)

Journal Pre-proof

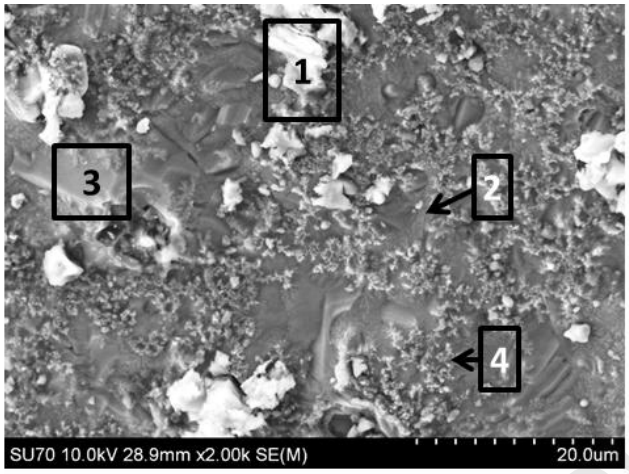

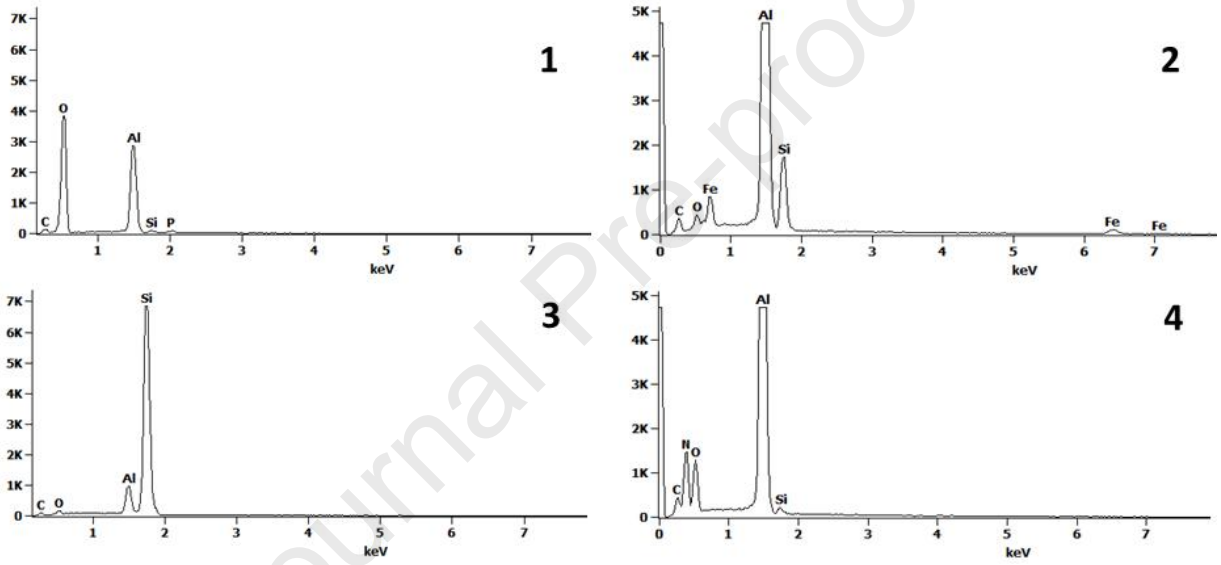

Journal Pre-proof

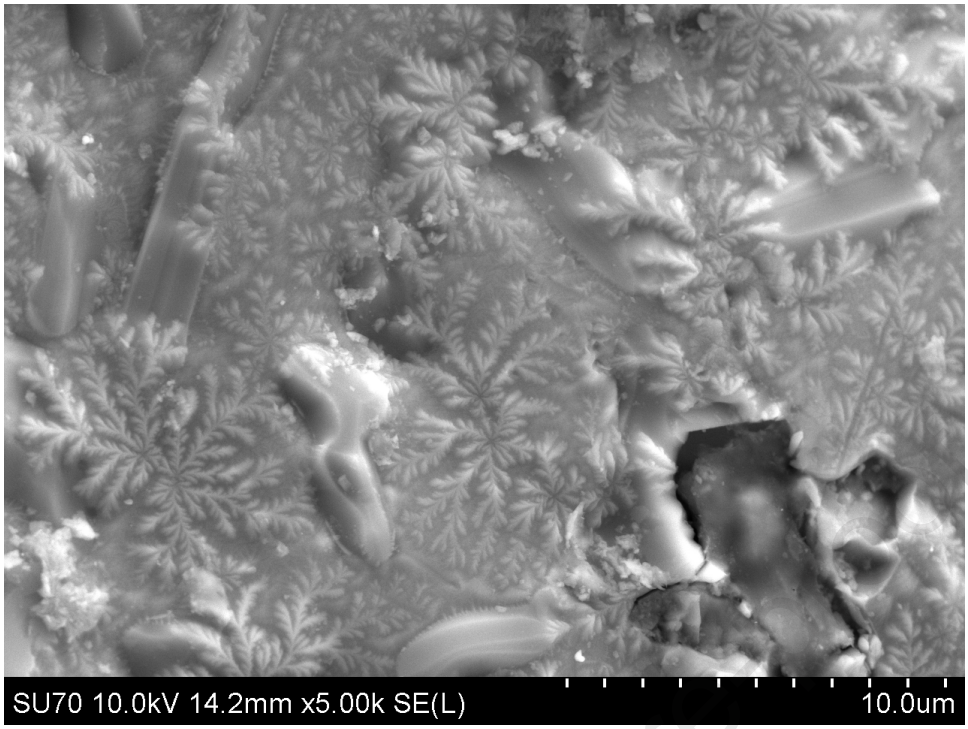

Journal Pre-proof

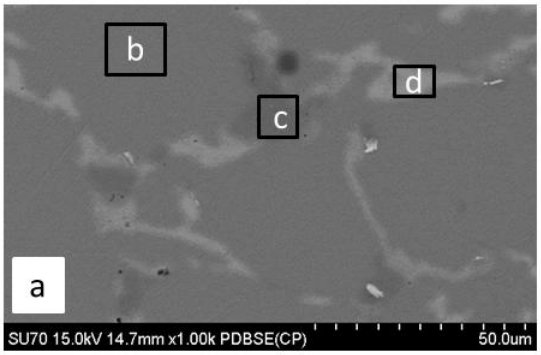

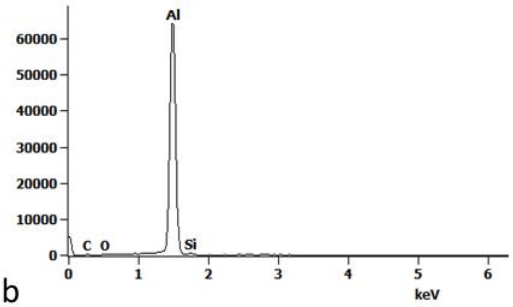

b

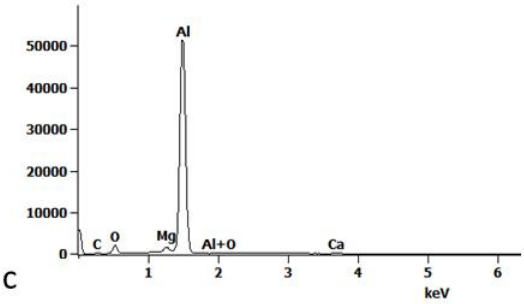

c

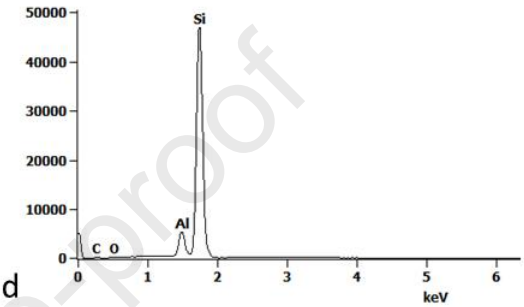

d

Journal Pre-proof

t= 0; T= 298 K

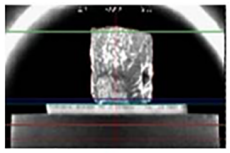

t= 3 min; T~ T_m

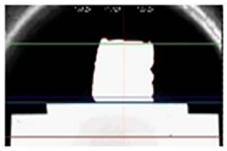

t= 18 min; T> T_m

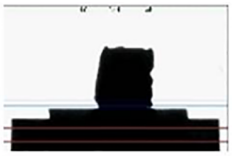

t= 30 min; T~ T_f

Journal Pre-proof

Journal Pre-proof

Figure 1. SEM image of SLMed AlSiMg showing the points for EDXS measurements; 1- representative EDX spectra of the Al matrix, 2- the cellular Si rich network, and 3- a thin oxide layer with also Mg. Spectra were cropped at the same count number in order to highlight the difference between Si, O and Mg relative content.

Figure 2. Cross section of the SLMed AlSiMg alloy indicating the presence of oxides layers surrounding previous melting pools or balling liquid (left); EDXS compositional analysis related to the points 1-2. Spectra were cropped at the same count number in order to highlight the difference between O and Mg relative content (right).

Figure 3. Contact angle versus time of SLMed AlSiMg alloy on Al_2O_3 substrate under vacuum (P= 10^{-2} Pa).

Figure 4. Evolution of the SLMed AlSiMg sample on Al_2O_3 substrate during the wetting test shown in Figure 3 (t= time; T_m = melting temperature; T_f= final temperature).

Figure 5. Lateral (a) and top (b) views of the AlSiMg drop solidified on the Al_20_3 substrate after the wetting test under vacuum.

Figure 6. SEM micrograph of the surface of the AlSiMg drop solidified on the Al_20_3 substrate after the wetting test under vacuum condition, lower part of the specimen. Typical features are highlighted in the micrographs and corresponding typical EDXS analyses are reported: 1- blocky aluminum oxides, 2- iron rich particles, 3-silicon particles, 4-small globular nitrogen rich aluminum oxides.

Figure 7. SEM micrograph of the surface of the AlSiMg drop solidified on the Al_2O_3 substrate after the wetting test under vacuum condition: leaf like oxides are visible, together with Silicon particles emerging from inside.

Figure 8. SEM image of the sample's section, showing the EDXS measurement areas (a); EDXS spectra representative of the three regions (b-d).

Figure 9. Evolution of the SLMed AlSiMg alloy on Al_2O_3 substrate during the wetting test performed under Ar atmosphere (t= time; T_m = melting temperature; T_f= final temperature).

Journal Pre-proof

Figure 10. Image of the SLMed AlSiMg sample solidified on Al_2O_3 substrate, after the end of the wetting test performed under Ar atmosphere.

Figure 11. Micrographs of the drop surface of SLMed AlSiMg alloy on Al_2O_3 substrate after the wetting test performed under Ar atmosphere low (left) and high (right) magnification.

Figure 12. SEM image of the Al_2O_3 substrate after the wetting test performed under Ar atmosphere; spectrum of the polygonal aluminum oxides (1) and the thin mixed aluminium-silicon oxide (2).

Figure 13. Surface tension isotherms of liquid Al-Si alloys calculated for T=1100 °C (full line – Butler's model; dashed line – the ideal solution model) together with the literature data (▲) [45]. For a comparison, an estimation of the surface tension of the Al-10Si-0.4Mg (Al-9.64Si-0.45Mg, in at %) given by the surface tension calculated value of the Al89.91-Si10.09 (line 1 – compositional location of the Al89.91-Si10.09 alloy).

Figure 14. Surface segregation isotherms of liquid Al-Si alloys calculated for T=1100 °C (full line – Butler's model; dashed line – the ideal solution model). For a comparison, an estimation of the surface enrichment of the Al-10Si-0.4Mg (Al-9.64Si-0.45Mg, in at %) given by the corresponding value of the Al89.91-Si10.09 alloy (line 1 – compositional location of the Al89.91-Si10.09).

Journal Pre-proof

Journal Pre-proof

Highlights

- Vaporization of Mg in AlSiMg alloy is highlited
- Wettability of binary AlSi and SLM ASiMg alloys show comparable contact angles value
- Strong surface oxydation under Ar athmosphere at high temperature in SLM produces oxide layers at solidified melting pools interphases

Journal Pre-proof

Journal Pre-proof

Declaration of interests

☒ The authors declare that they have no known competing financial interests or personal relationships that could have appeared to influence the work reported in this paper.

☐The authors declare the following financial interests/personal relationships which may be considered as potential competing interests:

Pontida, 08 May 2020

Ausonio Tuissi

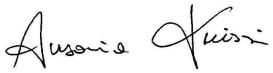

Journal Pre-proof

Journal Pre-proof

Declaration of interests

☒ The authors declare that they have no known competing financial interests or personal relationships that could have appeared to influence the work reported in this paper.

☐The authors declare the following financial interests/personal relationships which may be considered as potential competing interests:

09/05 2020, Carlo Alberto Biffi

Journal Pre-proof

Journal Pre-proof

Declaration of interests

☒ The authors declare that they have no known competing financial interests or personal relationships that could have appeared to influence the work reported in this paper.

☐The authors declare the following financial interests/personal relationships which may be considered as potential competing interests:

Lecco, 08 / Mag/ 2020, Paola Bassani

Journal Pre-proof

Journal Pre-proof

Declaration of interests

☒ The authors declare that they have no known competing financial interests or personal relationships that could have appeared to influence the work reported in this paper.

☐The authors declare the following financial interests/personal relationships which may be considered as potential competing interests:

DONATELLA GIURANNO
08/05/2020

Journal Pre-proof

Journal Pre-proof

Declaration of interests

☒ The authors declare that they have no known competing financial interests or personal relationships that could have appeared to influence the work reported in this paper.

☐The authors declare the following financial interests/personal relationships which may be considered as potential competing interests:

Enrica Ricci

Genoa, May 8,2020

Journal Pre-proof

Journal Pre-proof

Declaration of interests

☒ The authors declare that they have no known competing financial interests or personal relationships that could have appeared to influence the work reported in this paper.

☐The authors declare the following financial interests/personal relationships which may be considered as potential competing interests:

Lecco, 08-05-2020

Jacopo Fiocchi

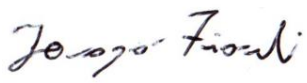

Journal Pre-proof